The feasibility of MT tipper data to monitor CO2 storage sites

Colton Kohnke, Yaoguo Li, Center for Gravity, Electrical, and Magnetic Studies, Colorado School of Mines*
Richard W. Hammack, National Energy Technology Laboratory, U.S. Department of Energy

SUMMARY

Monitoring carbon storage sites using geophysical techniques is a critical component to the success and safety of storage programs. Currently, the primary methods of monitoring such sites are seismic and, to a much lesser extent, electromagnetics using active sources. The cost of such methods, especially seismic, can be prohibitively expensive . Natural source electromagnetics, or magnetotellurics (MT), represents a low-cost, and underutilized method with the potential to aid CO_2 monitoring efforts. Specifically, the tipper of MT data gives insight to the dimensionality of the subsurface and is able to detect the expansion front of a CO_2 plume in a saline reservoir. We analyze the feasibility of using the tipper to monitor two shallow CO_2 plumes and conclude that the tipper may be a suitable method for long-term monitoring.

INTRODUCTION

Storing carbon dioxide (CO_2) in geologic formations is a way to reduce CO_2 in the atmosphere and mitigate the effects of climate change. These storage sites need to be monitored to ensure the integrity of the injection site, but also to satisfy regulatory requirements of up to 80 years of monitoring post injection (Benson et al., 2005). Geophysics plays an important role in monitoring efforts, but the cost of repeated surveys can be unappealing to site operators. Therefore, low-cost geophysical methods such as the electromagnetic (EM) methods have an opportunity to fill the gap for monitoring. However, there are few studies that evaluate the feasibility of using EM methods for monitoring purposes.

The EM method we focus on in this paper is magnetotellurics (MT), also called natural source electromagnetics. MT uses natural fields as a source and records the magnetic and electric fields at the surface. In a typical MT survey, the horizontal components of the electric field are measured at the surface using electric dipole receivers, and the horizontal and vertical components of the magnetic field are measured using directional magnetometers. Both fields are then combined in the frequency domain to calculate an impedance tensor (Z), and the components of the magnetic field are combined to form the tipper (T). The impedance and tipper can then be inverted for a resistivity model of the subsurface.

MT has shown promise in carbon storage scenarios. Ogaya et al. (2014) and Beka et al. (2017) shows that MT in combination with other methods, such as time-domain EM and seismic, can create a baseline geoelectric model of the reservoir pre-injection. Similarly, McLeod et al. (2018) uses multiple 1D MT soundings to recover large-scale resistivity information about the subsurface pre-injection. Streich et al. (2010) performs a modeling study of the electric field component of controlled-source MT, and shows that resistive post-injection reservoir structures can be detected by analyzing the vertical electric field (from a dipole receiver in a borehole). They conclude that the horizontal electric fields on the surface are generally insufficient to image a CO_2 plume without additional information.

There has been a recent interest in installing permanent geophysical monitoring sites utilizing EM receivers that only measure the magnetic field, as opposed to measuring both the electric and magnetic fields. This focus on magnetics stems from the installation and maintenance cost of establishing permanent electric field receivers. MT tipper surveys can also be readily deployed at permanent EM monitoring sites. For instance, consider a CO_2 storage site with a permanently installed time-domain EM transmitter loop and three-component magnetometer receivers. The main survey at the site may be the time-domain EM, but because the receivers are permanent and can record independent of the transmitter, they can measure the MT magnetic field when a time-domain EM survey is not being conducted. By only measuring the MT magnetic field we lose access to the impedance tensor, but retain the tipper data. The value of the tipper by itself is rarely discussed in MT problems, and is often ignored in favor of the information gained from the impedance tensor. However, results from recent work with ZTEM data (Izarra et al., 2011) suggests that tipper data can be used to gain insights about the subsurface. Surveys that measure the tipper can also be used in conjunction with other electromagnetic methods to improve the understanding of the reservoir.

This paper focuses on the information that can be obtained from using the tipper data in the absence any other data. We first provide an overview of the information content related to the tipper, and then analyze modeling examples of using the tipper in two reservoir scenarios.

MT TIPPER DATA

Let us consider a MT tipper survey. The source term is an electromagnetic plane-wave of unknown strength transmitted vertically into the subsurface. The source frequencies below 1 Hz are generated by solar winds interacting with the Earth's magnetic field. Frequencies above 1 Hz are generated by lightning strikes interacting with the ionosphere. The receivers measure the three-components of the magnetic field at the surface. Since the strength of the source signal is unknown, we compute the two components of the tipper (T_{zx}, T_{zy}) as a ratio of

the measured magnetic field (**H**) components,

$$T_{zx} = \frac{H_y^{(y)} H_z^{(x)} - H_y^{(x)} H_z^{(y)}}{H_x^{(x)} H_y^{(y)} - H_x^{(y)} H_y^{(x)}} \tag{1}$$

$$T_{zy} = \frac{H_x^{(x)} H_z^{(y)} - H_x^{(y)} H_z^{(x)}}{H_x^{(x)} H_y^{(y)} - H_x^{(y)} H_y^{(x)}}, \tag{2}$$

where superscripts (x) and (y) denote the polarization of the field (Vozoff, 1972; Labson et al., 1985). A total tipper can then be formed by taking the L2-norm of the amplitude of each component of the tipper

$$T = \sqrt{T_{zx}^2 + T_{zy}^2}. \tag{3}$$

The tipper describes a tilt to the magnetic field as the plane wave interacts with conductivity structures in the subsurface. A common application of the tipper is a qualitative assessment of how well the subsurface can be represented by 1D layering. Due to the vertical plane-wave source, the vertical component of the magnetic field (and thus the tipper) will be zero for a 1D subsurface. Therefore the tipper can be used as a measurement of subsurface dimensionality. While the subsurface is not 1D, many candidate sites for carbon storage, such as the Aquistore site (Roach et al., 2014) and the Illinois Basin (McBride et al., 2020), can be approximated by 1D layering.

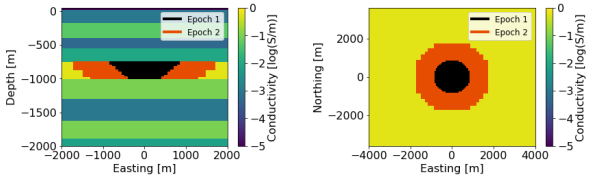

Figure 1: The baseline conductivity model with the extent of the CO_2 plume in both epochs overlaid in the reservoir layer viewed in (a) cross-sectional view at 0 m Northing and (b) a depth slice at 800 m.

In the context of a CO_2 plume expanding in a layered subsurface, both T_{zx} and T_{zy} are expected to be zero directly above the CO_2 plume and above the layered background. However, if measurements are taken above a region where the CO_2 contacts the saline reservoir, the tipper will be non-zero. Successive surveys above this region can then reveal the expansion front of the CO_2 plume as it mixes with and displaces the saline reservoir.

The depth of investigation of the tipper signal can be approximated from the recorded frequency (f) and the skin depth equation,

$$\delta = 503\sqrt{\frac{\rho}{f}}, \tag{4}$$

where ρ is halfspace resistivity. The resistivity and reservoir depth are site dependent. As an example, a target reservoir at 800 m depth, where CO_2 generally becomes supercritical in formation (White et al., 2003), and an average halfspace resistivity of 10 Ωm, will primarily require a signal at 2.5 Hz and below.

To illustrate the feasibility of using tipper data in an injection setting, we consider two models of CO_2 plume evolution. The first is a circular disk-like model expanding in the reservoir from the injection point. The second model has a plume that expands primarily in the north and south, simulating a reservoir with geologic constraints limiting the expansion in the east and west directions.

CIRCULAR PLUME IN A LAYERED SUBSURFACE

The first conductivity model is shown in Figure 1. The model consists of resistive 1D layering above and below a 200 m thick conductive saline reservoir starting at 800 m depth. The baseline model pre-injection represents the reservoir as a conductive 1D layer. Epochs 1 and 2 represent the 3D reservoir after injection events and are modeled by a two-phase system: the conductive saline reservoir being displaced by, and mixing with, the resistive super-critical CO_2 plume. The resistivity of the CO_2 plume in both epochs is modeled as 100 Ωm.

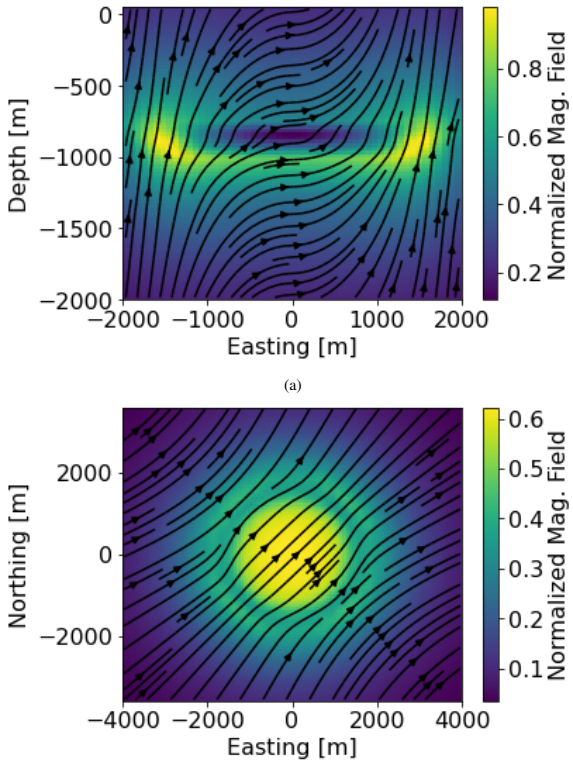

Figure 2: Normalized amplitude of the secondary magnetic field for epoch 2 at 1 Hz viewed in (a) cross-sectional view and (b) a depth slice at 800 m. Black arrows denote field direction and color denotes field strength.

To conduct the modeling of the MT fields, we separate the problem into a primary-secondary formulation. The primary

field is from the background model that is equivalent to the 1D baseline model. The primary magnetic field in the subsurface is purely horizontal due to the 1D layering of the background model and MT plane-wave source. The secondary magnetic field is then the field due to changes from the background model, such as from the resistive plumes in epochs 1 and 2.

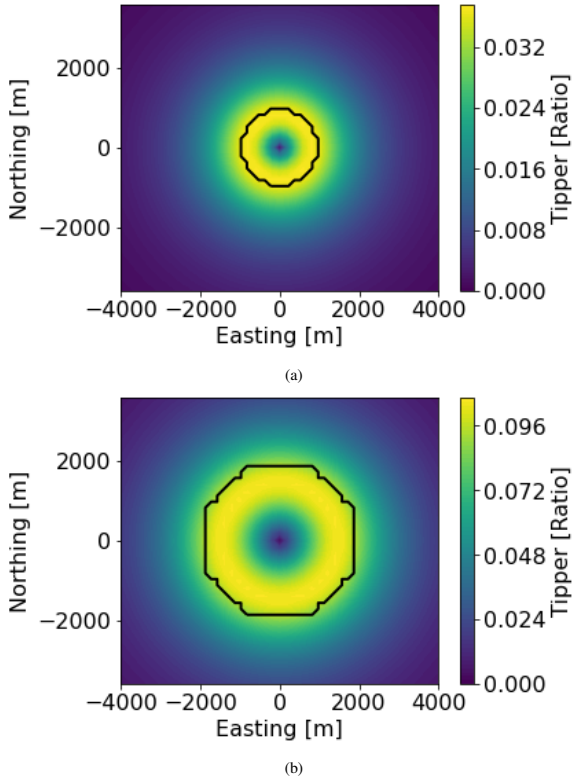

Figure 3: 1 Hz total tipper data at the surface receivers during (a) epoch 1, and (b) epoch 2. The black contour line denotes the edge of the CO_2 plume at 800 m depth.

To visualize the modeled secondary magnetic fields we model a plane-wave source rotated at 45° from North and compute the amplitude of each magnetic field component. Using this source is similar to showing both the magnetic field polarizations, and the total illumination they create. The obtained magnetic field has features from both polarizations, and shows how the inclusion of a resistive body influences the shape of the magnetic field. The shape of the magnetic field can then be translated to how the tipper changes over the CO_2 plume.

The amplitude of the secondary magnetic field modeled using epoch 2 at 1 Hz is shown in Figure 2, and the influence of the CO_2 plume can clearly be seen. The magnetic field is shown to be high at the edges of the plume, and low inside the plume. This is expected as the horizontal telluric currents in the subsurface are deflected by the resistive zone, increasing the current density near the conductivity boundary, and therefore increasing the strength of the magnetic field. Since the layer above the reservoir is more resistive than the layer below, more current diverts into the lower layer to avoid traveling through the resistive plume in the reservoir. At the edges

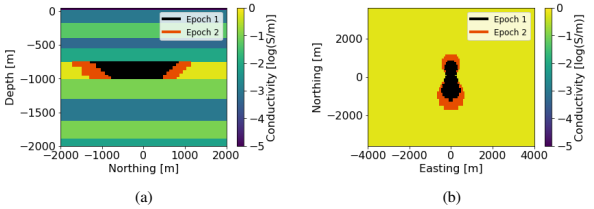

Figure 4: The conductivity model with the extent of CO_2 plume in both epochs overlaid in the reservoir layer viewed in (a) cross-sectional view and (b) a depth slice at 800 m.

of plume, the magnetic field is shown to have a significant vertical component, which means that the measured tipper data will be non-zero near the edge of the plume. Over the middle section of the plume, the magnetic field is primarily horizontal, which will result in a zero tipper.

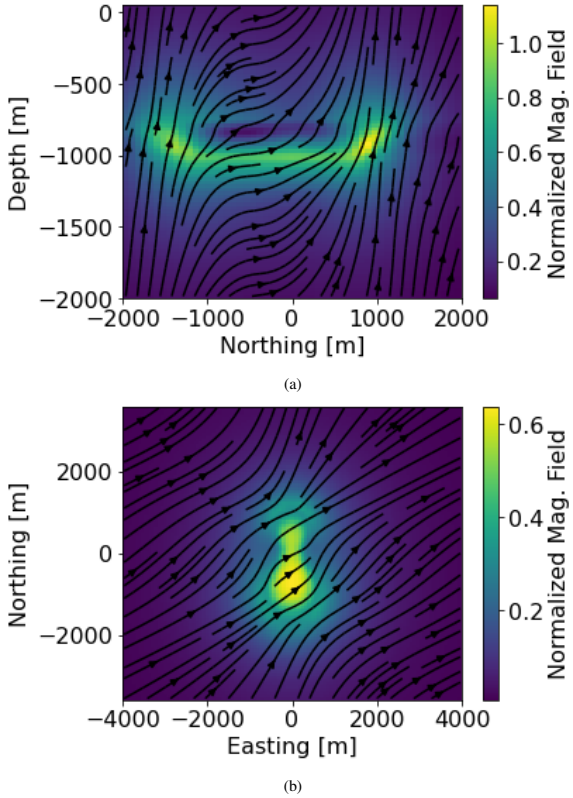

Figure 5: Normalized amplitude of the secondary magnetic field for epoch 2 at 1 Hz viewed in (a) cross-sectional view at 0 m Easting and (b) a depth slice at 800 m. Black arrows denote field direction and color denotes field strength.

The total tipper data at the surface for both epochs at 1 Hz is shown in Figure 3. The total tipper is zero directly above the center of the injected CO_2, and increases in strength towards the contact with the conductive background, before returning to zero. The tipper is also able to approximate the edge of the CO_2 plume. Between epochs, the zero region in the center grows, indicating an expansion to the local 1D structure of the

subsurface. The tipper also increases in size and strength in epoch 2, indicating stronger vertical magnetic fields resulting from more currents being deflected by a larger resistive body in the subsurface. The modeled magnitude of the tipper is similar to values recorded during ZTEM surveys in Izarra et al. (2011) and Yang et al. (2019), which gives confidence that a MT tipper survey could be used in the presented scenario and recover meaningful results.

ELONGATED PLUME IN A LAYERED SUBSURFACE

The second model we analyze represents a CO_2 plume that expands primarily in a single direction and develops two uneven lobes along that expansion path. Cross-sections of the baseline model and both epochs is shown in Figure 4.

The amplitude of the secondary magnetic field for epoch 2 at 1 Hz is shown in Figure 5. Again, we notice the secondary magnetic fields are strongest at the edge of the resistive body, and are low inside the resistive zone. The fields are shown to be diverting around the resistive zone. Even though the thickness of the plume in the easting direction is minimal, the magnetic field is shown to be diverting around the zone in the depth section.

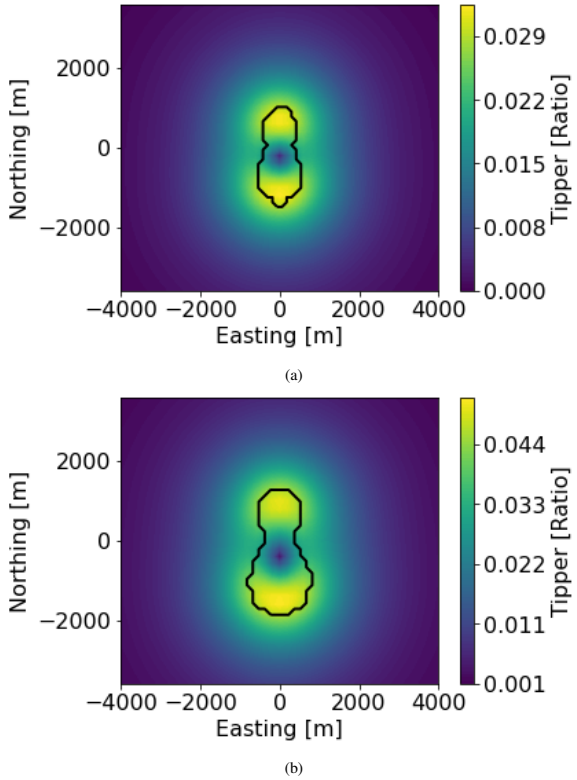

Figure 6: Total tipper data measured at the receivers during (a) epoch 1, and (b) epoch 2. The black contour line denotes the edge of the CO_2 plume at 800 m depth.

The total tipper at the surface in Figure 6 shows that the edges of the CO_2 plume contacting the background produces a strong tipper response. Due to the plume's shape being elongated in the Northing ($\hat{x}$) direction, the T_{zx} component of the tipper is stronger than the T_{zy} (corresponding to Easting, $\hat{y}$). This results in a stronger total tipper response at the North and South boundaries of the plume, but the East and West boundaries can still be discerned from the data.

CONCLUSION

The MT tipper is often ignored in favor of working with the impedance tensor and apparent resistivity values. When the tipper is used, it is frequently to identify conductive anomalies in the subsurface as opposed to resistive anomalies. However, we have shown that the tipper can play a role in the underground carbon storage problem, where it can be used to delineate the boundary between a resistive plume and a more conductive saline layer. This is due to the fact that the tipper is sensitive to non-1D structure in the subsurface. Successive surveys after multiple injection events can result in a way to track the CO_2 as it expands within the conductive saline layer. Time-lapse tipper data, as well as combining tipper data with other geophysical investigations, may also provide a way to gain further insight into the evolution of the CO_2 plume at the site.

ACKNOWLEDGMENTS

The support for this work was provided by the U.S. Department of Energy, National Energy Technology Laboratory under carbon storage advanced R&D. The authors thank the SimPEG project for the finite volume MT code (Heagy et al., 2017).

REFERENCES

Beka, T. I., K. Senger, U. A. Autio, M. Smirnov, and Y. Birkelund, 2017, Integrated electromagnetic data investigation of a Mesozoic CO2 storage target reservoir-cap-rock succession, Svalbard: Journal of Applied Geophysics, **136**, 417–430.

Benson, S., G. Hoversten, E. Gasperikova, and M. Haines, 2005, Monitoring protocols and life-cycle costs for geologic storage of carbon dioxide, *in* Greenhouse Gas Control Technologies 7: Elsevier, 1259–1264.

Heagy, L. J., R. Cockett, S. Kang, G. K. Rosenkjaer, and D. W. Oldenburg, 2017, A framework for simulation and inversion in electromagnetics: Computers & Geosciences, **107**, 1–19.

Izarra, C., J. Legault, and C. Fontura, 2011, ZTEM airborne tipper AFMAG results over the Copaquire Porphyry, northern Chile: 12th International Congress of the Brazilian Geophysical Society & EXPOGEF, Rio de Janeiro, Brazil, 15–18 August 2011, Brazilian Geophysical Society, 1154–1157.

Labson, V. F., A. Becker, H. F. Morrison, and U. Conti, 1985, Geophysical exploration with audiofrequency natural magnetic fields: Geophysics, **50**, 656–664.

McBride, J. H., H. E. Leetaru, J. T. Freiburg, and S. G. Whittaker, 2020, Precambrian structure revealed by CCS seismic profiles from the Illinois Basin: SEG Technical Program Expanded Abstracts 2020, Society of Exploration Geophysicists, 1125–1129.

McLeod, J., I. Ferguson, J. Craven, B. Roberts, and B. Giroux, 2018, Pre-injection magnetotelluric surveys at the Aquistore CO2 sequestration site, Estevan, Saskatchewan, Canada: International Journal of Greenhouse Gas Control, **74**, 99–118.

Ogaya, X., P. Queralt, J. Ledo, Á. Marcuello, and A. G. Jones, 2014, Geoelectrical baseline model of the subsurface of the Hontomín site (Spain) for CO2 geological storage in a deep saline aquifer: A 3D magnetotelluric characterisation: International Journal of Greenhouse Gas Control, **27**, 120–138.

Roach, L. A. N., D. White, and B. Roberts, 2014, An assessment of the time-lapse seismic repeatability using a permanent array for reservoir monitoring at the Aquistore CO 2 storage site, Saskatchewan, Canada: SEG Technical Program Expanded Abstracts 2014, Society of Exploration Geophysicists, 4924–4929.

Streich, R., M. Becken, and O. Ritter, 2010, Imaging of CO2 storage sites, geothermal reservoirs, and gas shales using controlled-source magnetotellurics: Modeling studies: Geochemistry, **70**, 63–75.

Vozoff, K., 1972, The magnetotelluric method in the exploration of sedimentary basins: Geophysics, **37**, 98–141.

White, C. M., B. R. Strazisar, E. J. Granite, J. S. Hoffman, and H. W. Pennline, 2003, Separation and Capture of CO 2 from Large Stationary Sources and Sequestration in Geological Formations—Coalbeds and Deep Saline Aquifers: Journal of the Air & Waste Management Association, **53**, 645–715.

Yang, D., D. Fournier, S. Kang, and D. W. Oldenburg, 2019, Deep mineral exploration using multi-scale electromagnetic geophysics: the Lalor massive sulphide deposit case study: Canadian Journal of Earth Sciences, **56**, 544–555.